Journal of Nuclear Materials 405 (2010) 44–49

Contents lists available at ScienceDirect

Journal of Nuclear Materials

journal homepage: www.elsevier.com/locate/jnucmat

Evaluation of creep damage in a welded joint of modified 9Cr–1Mo steel

Yongkui Li [a,*], Yoshio Monma [b], Hiromichi Hongo [c], Masaaki Tabuchi [c]

[a] Research Group for Nuclear Materials Modeling, Japan Atomic Engineering Agency, Tokai 319-1195, Japan
[b] Environmental Systems Engineering Course, Kochi University of Technology, Kami 7820053, Japan
[c] High Temperature Material Group, National Institute for Materials Science, Tsukuba 3050047, Japan

ARTICLE INFO

Article history:
Received 30 November 2009
Accepted 21 July 2010

ABSTRACT

This paper aims to evaluate the creep damage of modified 9Cr–1Mo steel under 600 °C operating conditions, using constitutive equations based on the continuum damage mechanics. The accumulation of voids over a long period is believed to contribute to the formation of Type IV cracking, which in turn leads eventually to the failure of weldment under conditions of higher temperatures and lower stresses. Specimens of base metal, a simulated fine-grained heat affected zone, and a thin (thick) welded joint were kept under stress from 80 to 160 MPa at 600 °C. During the creep tests of thick plate welded joint specimens, the application of stress was suspended several times, and the creep damage as indicated by the void distribution was examined quantitatively using a laser microscope. The combined effect of the equivalent creep strain and the stress triaxial factor was considered and introduced into the constitutive equations with the aid of a finite element method. The logarithms of m and $1/\lambda$ in the continuum damage mechanics equations were determined to have a linear correlation with the ratio of the applied stress to the yield stress for homogeneous materials. In this way, the damage distribution and evolution in the fine-grained heat affected zone were evaluated successfully.

1. Introduction

9Cr heat resistant steel is normally used in the header plate in thermal power plants, considering its low stress mechanical properties and its cost. However, it is well known that long term exposure at elevated temperatures leads to cracking, due to the Type IV weldment zone damage involving void coalescence [1,2]. There have been some studies of the damage processes. In these studies, the evaluation equations, which are most popular, are those including a continuum damage mechanics (CDM), which were first proposed by Kachanov [3] and subsequently modified by other researchers [4–7]. Development of the continuum damage mechanics is normally divided into two categories, that for macroscopic damage and microscopic damage [8]. So far most of the evaluation studies have been conducted on homogeneous materials. However, these evaluation methods of the weldment have practical difficulties because of their complexity, requiring much expense and time. Also, we need to consider that a multiaxial stress state always exists in the complicated structures of a weldment. In additional equations supplementing the CDM an invariable multiaxial stress state was assumed for a given material in the conventional constitutive equations [9,10]. However, this assumption is not valid in a finite element method (FEM). In a FEM calculation, the multiaxial stress state is very sensitive to the groove shape for a weldment and also it varies with the location. Therefore, it cannot be a good indicator of the creep damage distribution, and can only predict the rupture life. Moreover, the material constants in the conventional constitutive equations cannot flexibly model the creep behavior under different stress levels. In this paper, we propose modified CDM equations to evaluate the damage distribution and evolution in a weldment which take the combined effect of equivalent creep strain and stress triaxial factor along the weak region of the heat affected zone (HAZ) into account.

2. Constitutive damage equations

The traditional CDM constitutive equations for creep damage evaluation are normally shown as Eqs. (1) and (2) [10–13] in form:

$$d\omega/dt = M[\alpha\sigma_1 + (1-\alpha)\sigma_{eq}]^{\chi} t^{m-1} f^{*}/[(1+\varphi)(1-\omega)^{\varphi}] \quad (1)$$

$$d\omega/dt = 1.5A\sigma_{eq}^{n-1} S_{ij} t^{m-1}/(1-\omega)^{n} \quad (2)$$

In the equations, σ_{eq} is the equivalent creep stress, and σ_1 is the maximum principal stress. Both of σ_{eq} and σ_1 are variable with changing of not only locations in complicated components (such as a welded joint) but also time during creep [14]. The changes of the two stresses make the calculation difficult in the traditional evaluation equations. Therefore, we made the modifications by substitution of the term of $(\alpha\sigma_1 + (1-\alpha)\sigma_{eq})$ in Eq. (1) and σ_{eq} in Eq. (2)

* Corresponding author. Address: Research Group for Nuclear Materials Modeling, Nuclear Science and Energy Directorate, Japan Atomic Energy Agency (JAEA), 2-4 Shirakata, Shirane, Tokai-mura, Naka-gun, Ibaraki-ken 319-1195, Japan. Tel.: +81 29 282 6373; fax: +81 29 282 6380.
E-mail addresses: li.yongkui@jaea.go.jp, liyongkuixd@gmail.com (Y. Li).

0022-3115/$ - see front matter © 2010 Elsevier B.V. All rights reserved.
doi:10.1016/j.jnucmat.2010.07.033

Table 1
Chemical compositions of the BM and welding filler (mass%).

Compositions	C	Si	Mn	P	S	Cr	Mo	V	Nb	N	Al	Cu	Ni
Base metal	0.1	0.25	0.43	0.006	0.002	8.87	0.93	0.19	0.07	0.06	0.014	0.012	0.06
Weld filler	0.08	0.12	1.02	0.005	0.004	8.99	0.9	0.18	0.04	–	–	0.12	0.71

with the applied stress σ_0 to simplify the calculation of evaluation of creep damage. Moreover, the traditional CDM constitutive equations can only give a global evaluation curve with creep time. We made the continuous modifications on the traditional CDM constitutive equations with introducing an exponential function f^* to evaluate not only creep damage but also the damage distribution in the crossing section of the creep specimens, and they are shown as the following equations:

$$d\omega/dt = M\sigma_0^{\chi} t^{m-1} f^* / [(1+\varphi)(1-\omega)^{\varphi}] \quad (3)$$

$$d\varepsilon/dt = 1.5A\sigma_0^{n-1} S_{ij} t^{m-1}/(1-\omega)^n \quad (4)$$

where ω represents the scalar quantity of damage in the range from 0 at the beginning of damage formation to 1 at failure, ε is the strain, t is the time, S_{ij} is the deviator, and σ_0 is the external force applied on the specimens. Other coefficients and exponents such as n, A, χ and M are the material constants, and are independent of stress in conventional evaluation equations. m and φ are dependent on the applied stress.

The f^* in Eq. (3) is dependent on the equivalent creep strain and stress triaxial factor during creep. The combined effect of the equivalent creep strain and the stress triaxial factor was clarified to accelerate the nucleation of voids in the FG-HAZ of Mod.9Cr–1Mo welded joint during creep [15,16]. Hence, the evaluation of the creep damage was conducted with f^* as a function of stress triaxial factor with power of equivalent creep strain introduced into the CDM equations, and f^* was defined as

$$f^* = TF^{C\varepsilon^*} \quad (5)$$

where TF is the stress triaxial factor [15], C is equal to 100 for the modified 9Cr–1Mo steel at 600 °C, and the factor ε^* denotes the equivalent creep strain. The function f^* can only reflect the distribution of creep damage along the profile of the FG-HAZ. When the specimen is homogenous, the equivalent creep strain is the same and the value of the stress triaxial factor is 1 at any location, so we could be sure that the inducing factor f^* was equal to 1 in the specimens of BM and simulated HAZ. However, f^* is variable in the FG-HAZ of a weldment under uniaxial tensile stress because the stress triaxial factor and equivalent creep strain are always changing with the location due to their sub-components having different mechanical properties. TF and ε^* in the welded joint were obtained by FE simulation with MARC software [16]. Thus f^* along the FG-HAZ can be calculated.

3. Experiment and simulation procedures

3.1. Creep tests and void observation

The material investigated in our study was Mod.9Cr–1Mo steel plate 25 mm in thickness, with the chemical compositions shown in Table 1. The plate was welded by the gas tungsten arc welding (GTAW) method with double U grooves. The post weld heat treatment (PWHT) adopted was to keep temperature at 745 °C for 1 h. The simulated HAZ specimens were produced by rapid heating (60 °C/s) to a peak temperature of 900 °C followed by gas cooling (40 °C/s) by a weld simulator. The round bar specimens with 4 mm in diameter and 15 mm in gauge length for simulated HAZ, those with 6 mm in diameter and 30 mm in gauge length for BM,

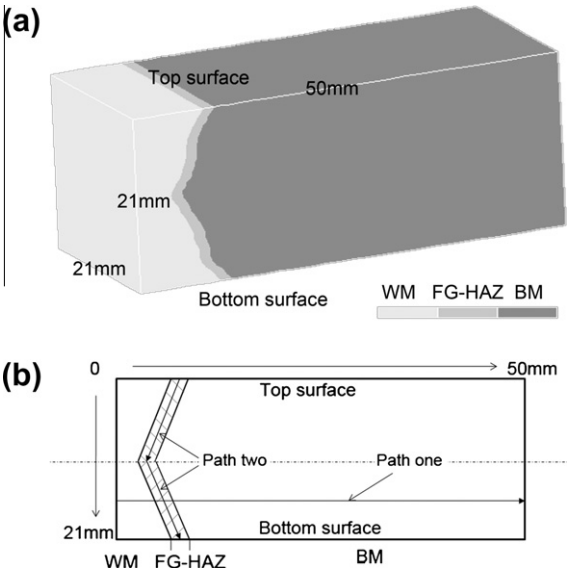

Fig. 1. Three-material and three-dimensional finite element model of thick plate welded joint specimen, and diagram of Path one and Path two in the central cross section.

and smooth thin plate specimens for the welded joint were machined and crept in long term at 600 °C with various stress levels from 80 MPa to 160 MPa. Several thick plate specimens with a geometry containing the welded joint shown in Fig. 1 were also machined. These thick plate specimens were crept at 600 °C by the applying stress of 90 MPa. The creep tests were interrupted at about 0.1, 0.2, 0.5, 0.7, 0.8 and 0.9 of the rupture life in order to observe the evolution of creep voids. More details of the experimental procedures can be found in our previous papers [16–18].

3.2. Two weldment simulation models

The three-material (BM, FG-HAZ and weld metal) and three-dimensional finite element model shown in Fig. 1 was constructed to calculate the stress–strain distributions in a thick plate welded joint specimen, for comparison with the above void measurement. This model had the dimensions $21 \times 21 \times 50$ mm, and was composed of 6660 elements and 8436 nodes. The width of the fine-grained HAZ was made 1.3 mm, based on microstructural observations. Details of this model also can be found in Ref. [16]. FEM simulation was also conducted on the thin welded joint with dimensions $17 \times 5 \times 50$ mm under the same temperature of 600 °C and applied stress of 90 MPa. The thin model was composed of 6560 elements and 8316 nodes. This had a weak HAZ (FG-HAZ) with the same width as the thick model due to the same welding processing. The mechanical parameters discussed later were all obtained along two paths in a central plane-traversing the weld metal (WM), the FG-HAZ, and the BM of the FEM model, as shown in the cross section diagram of Fig. 1. Path one ran at 1/4 the total height above the bottom surface, and Path two ran through the middle of the FG-HAZ part of the simulation model.

4. Results and discussion

4.1. Logarithms of m and $1/\lambda$ dependent on the applied stresses

To make characterization of later states easier, we introduced a temporary parameter λ defined as $\lambda = (\varphi + 1)/(\varphi + 1 - n)$ which used in the integrating continuum damage mechanics equations from Eqs. (3) and (4). By fitting to the experimental results from the homogeneous specimens of base metal (BM) and fine-grained HAZ (FG-HAZ) shown in Fig. 2a and b, the logarithmic values (with base number of 10) of m and $1/\lambda$ were found to be linear with the ratio of the applied stress to the yield stress σ_0/σ_y. These linear relations are shown in the following equations:

$$\log_{10}(m) = k_1\sigma_0/\sigma_y + b_1 \quad (6)$$

$$\log_{10}(1/\lambda) = k_2\sigma_0/\sigma_y + b_2 \quad (7)$$

where k_1, k_2, b_1 and b_2 are material constants, independent of the applied stress. σ_y is the yield stress of the material, and is obtained by a tensile test at the temperature of the evaluation.

The two logarithms of m and $1/\lambda$ in Eqs. (6) and (7) were fitted to the creep behavior experimental data normalized creep strain vs. normalized creep time for BM and FG-HAZ after Eqs. (3) and (4) integrating. As shown in Fig. 2, the logarithms of m and $1/\lambda$ increased in the applied stresses. The values of m and $1/\lambda$ were in the range from 0 to 1, but never reached these two end points. Moreover, the values of m and $1/\lambda$ for the simulated HAZ were larger than that of BM at the same stress levels. The numerator is smaller than the denominator in $(\varphi + 1 - n)/(\varphi + 1)$ therefore the factor φ is monotone with the applied stress because n is a material constant independent of the applied stress.

The two logarithms for weldments were obtained from the thick welded joint under 90 MPa at 600 °C. In the case of the thin welded joint, m might be slightly smaller than these obtained values while $1/\lambda$ might be larger due to the time to rupture and elongation of thick welded joint are higher than those of thin welded joint under 90 MPa at 600 °C. As shown in Fig. 3 the equivalent creep strain for thin welded joint was obtained by FEM at during creep under 90 MPa at 600 °C. The equivalent creep strain becomes larger in order of BM, WM and HAZ parts of the welded joint specimen. The equivalent creep strain in the BM of thin welded joint FE model is about 0.0002 at time 7200 h while we got the simulated data for thick welded joint FE model is 0.0025 at time of 8000 h in Fig. 12 of Ref. [16]. Therefore, the elongation for thick welded joint is testified to be larger than that thin welded joint by the FE simulation under same conditions. Though the equivalent creep strain for HAZ is lager for thin welded joint than that of the HAZ of thick welded joint, it can not affect the comparing results of rupture strain of thick and thin welded joint because it is a very narrow region (1.3 mm in width) in a welded joint. Because the available experimental data was insufficient, the logarithms of m and $1/\lambda$ under 90 MPa also were used for the welded joint at the other stress levels.

4.2. Global evaluation of strain and damage of BM, simulated HAZ and weldments

The parameters of materials in the CDM equations for the BM, simulated HAZ, and the welded joint (WJ) of the Mod.9Cr–1Mo steel at 600 °C are listed in Table 2. The material constants under two stress levels (110/130 MPa for BM and 80/100 MPa for simulated HAZ) were calculated. The prediction of creep strain was made for the BM and the simulated HAZ under several stress levels at 600 °C, as shown in Fig. 4. Generally speaking, the predictions were in good agreement with the measured creep strain except for the tertiary stages. However, the calculated strain by extrapolation under some stress larger than 130 MPa for BM and 100 MPa for HAZ are deviated somewhat due to the material degradation occurs in long term high temperature operation.

Fig. 5 shows the area fraction of voids (counted in observation by laser microscope) in the thick welded joint [16] and the evaluated damage factor by the present modified CDM equations under 90 MPa at 600 °C. The voids fraction is increasing with nominal creep time up to 0.008 mm^{-2} at about 0.91 of creep life. The

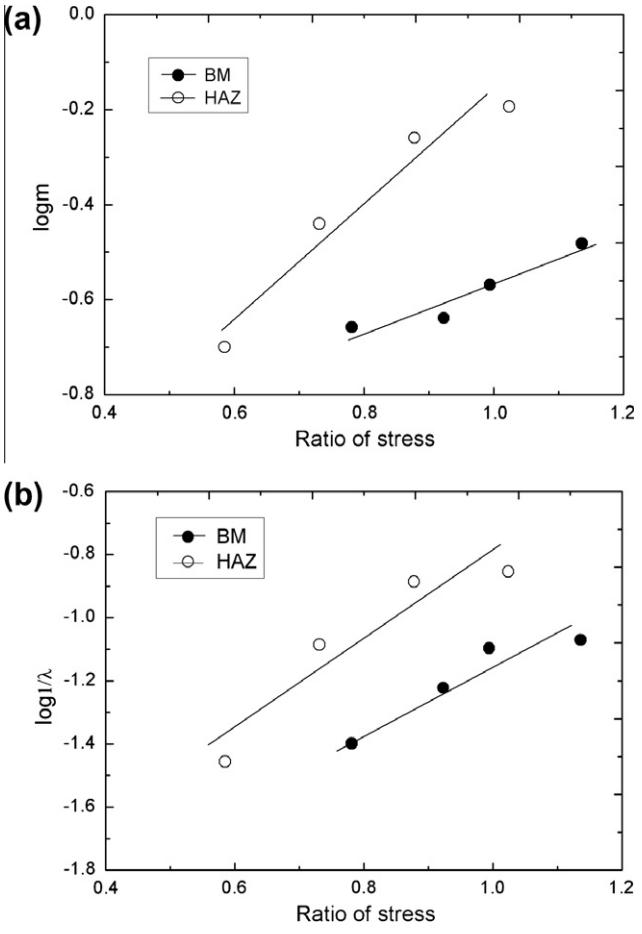

Fig. 2. Relations of logarithms of (m and $1/\lambda$) of BM and simulated HAZ with the ratio stress (σ_0/σ_y) at 600 °C.

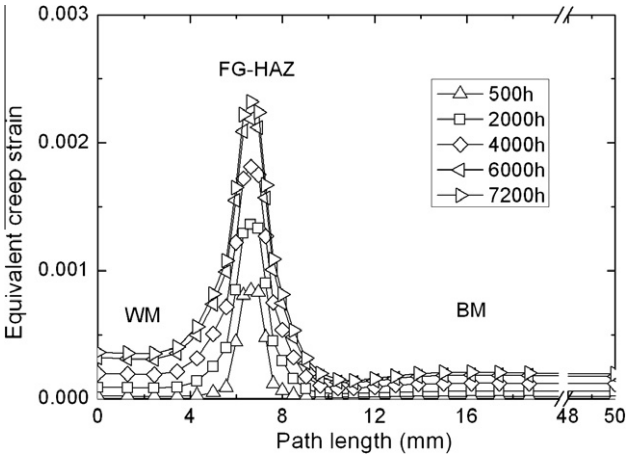

Fig. 3. Equivalent creep strain along Path one in thin welded joint welded joints under 90 MPa at 600 °C, calculated with FEM.

Table 2
Material constants for BM, Simulated HAZ, and WJ of the Mod.9Cr–1Mo steel at 600 °C.

Constants	BM	Simulated HAZ	WJ
s_y (MPa)	140.8	136.7	–
A	3.76E−12	1.44E−09	2.85E−07
n	4.7493	3.81	2.45
k_1	0.5415	1.159	–
k_2	0.954	1.3713	–
χ	0.4089	−0.055	0.6245
b_1	−1.08	−1.331	–
b_2	−2.111	−2.173	–
M (or Mf^*)	3.64E−03	4.04E−02	0.00244
m	–	–	0.14
φ	–	–	3.454

Note: The constant M is for the homogenous materials (such as BM and simulated HAZ), and Mf^* is for the WJ.

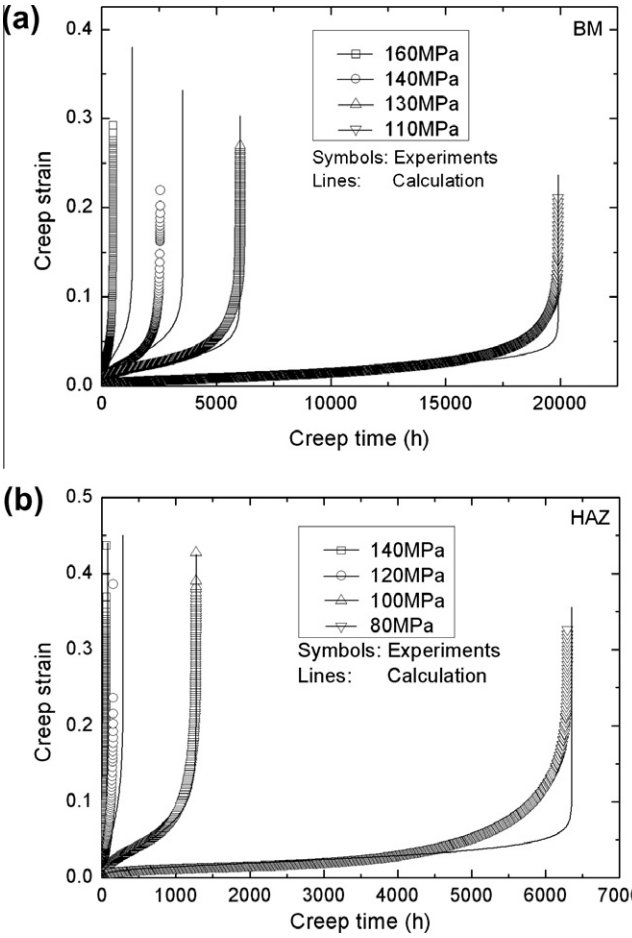

Fig. 4. Evaluation of creep strain evolution for (a) BM and (b) simulated HAZ under several stress levels at 600 °C.

evaluated damage is primarily composed of the void damage during creep. The evaluated curve shows more overestimate for damage of the creep specimen at earlier stage (before 0.23 of creep life) of creep time comparing creep fraction. For comparing with the creep void damage, the CDM constitutive equation needs to improve in future because the evaluating curve might consider too much strain hardening in primary stage.

Fig. 6 shows the predicted strain curves for the weldment against creep time under 80 MPa, 90 MPa, 100 MPa and 130 MPa

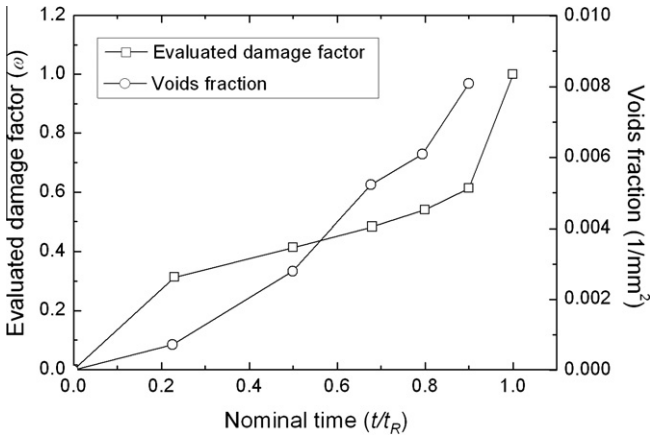

Fig. 5. Damage evolution predictions and experimental results (area fraction of voids) for a thick welded joint under 90 MPa at 600 °C.

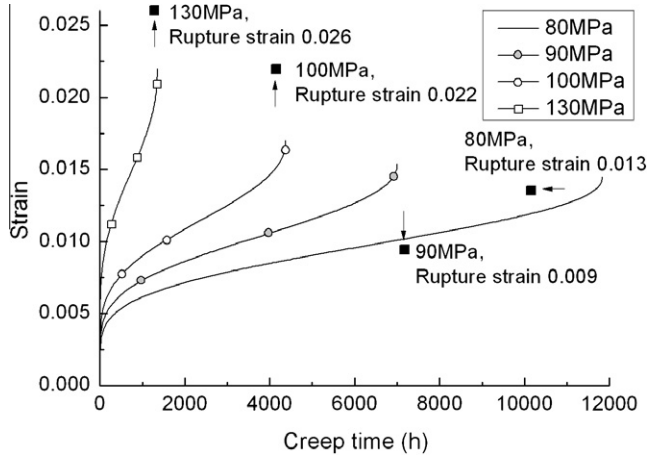

Fig. 6. Rupture strain in creep experiments and evaluated strain curves for thin weld joint at 600 °C.

at 600 °C. The calculated results are based on the thin welded joint specimen. The experimental results of rupture strain for the welded joints are 0.013, 0.009, 0.022 and 0.026 under 80 MPa, 90 MPa, 100 MPa and 130 MPa at 600 °C (as shown by the four solid square symbols in Fig. 6), respectively. The rupture strain for specimen under 90 MPa seems small too much, and which affected the evaluation of strain because we used extrapolation method for the rupture strain considering three stress levels (80/90/100 MPa) during evaluation. Rupture strain (0.0022 by evaluation) under the stress of 130 MPa is affected by the unexpected experimental rupture strain under 90 MPa. The factors of m and $1/\lambda$ affecting the trendlines of strain curve were obtained under 90 MPa. The others strain curves under 80 MPa, 100 MPa and 130 MPa also used the factors due to insufficient experimental results. Therefore the sufficient experimental results on strain data during creep can give the much accurate evaluating results. The present evaluation rupture strain is lower than rupture strain under 100 MPa, the increasing of factor A with the applied stress might give a much evaluation on rupture strain at stress higher than 100 MPa. As we had discussed Section 4.1, the creep strain calculated in thick welded joint is larger than that in thin welded joint specimen under 90 MPa at 600 °C. Therefore, the rupture strain of thick welded joint should be larger than that of thin welded joint. The modification by sub-

mitting σ_{eq} with σ_0 was believed no effects on the evaluation of strain. Though σ_0 is larger than σ_{eq}, the increasing of constant χ can remedy the effects bringing by stress term increasing in the modification.

4.3. Damage distribution in the profile of the FG-HAZ

Upon laser microscope observation, voids were mostly found in the weak HAZ with the small-size grains. The voids in the FG-HAZ grew up and connected each other after long term servicing at high temperatures, eventually leading to failure. In this section we evaluated the damage distribution and evolution within the weak HAZ of a welded joint, using the exponential function f^*. As mentioned above, the introduced exponential function f^* is a scalar quantity varying with location in the weak HAZ. It is introduced in consideration of the fact that the triaxial factor in combination with the equivalent creep strain promotes the failure of the thick welded joint at elevated temperatures. The data of equivalent creep strain and stress triaxial factor for the thick welded joint can be found in Figs. 15 and 16 in Ref. [16]. The primary purpose of this evaluation is to obtain the void distribution and the serious damage locations in the weak HAZ.

The final failure occurs due to the damage accumulation in all locations, and can be predicted referring to the term $\sigma^\wedge - \sigma_0/\sigma^\wedge$ in the weldment, where $\sigma^\wedge$ represents the break stress of the simulated HAZ. When the entire damage area fraction exceeds this ratio and then the damage factor ω is equal to 1, failure of the structure occurs. The predicted damage distributions and evolutions in the weak HAZ of a thick welded joint at 90 MPa and 600 °C are shown in Fig. 7. Damage factor was lower in both top and bottom surfaces while it was large in the locations close to those surfaces. This is corroborated by the fact that subsurface cracks are always found in weak HAZ after long term creep. The damage factors were a little lower near the center than in the subsurface locations. This diagram indicates that on a whole, the most critical damage was in the subsurface portions down to 20% of the length of Path two from the surface. Type IV cracks will be produced in these zones first.

In this diagram, the large damage is found in the two areas near to the top and bottom surfaces (0 mm/21 mm locations in HAZ respectively) of the weldment. Fig. 8a shows the distributions of the area fraction of creep voids in a HAZ along the thickness direction of the creep interrupted specimens, and Fig. 8b, taken by a laser microscope, illustrates the actual profile of creep damage in the weldment at 7970 h. A number of voids were found to focus in the up and lower 1/5 parts in the weak HAZ, moreover, obvious cracks appeared in the lower 1/5 part. The predicted damage distributions in Fig. 7 were in good agreement with the experimental results shown in Fig. 8a and the profile of a weak HAZ in Fig. 8b.

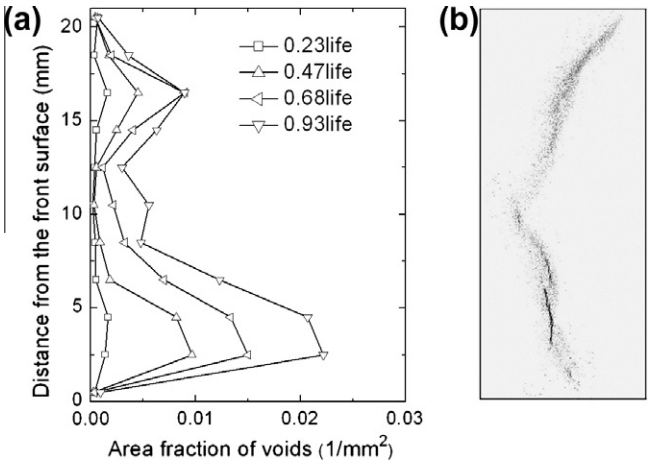

Fig. 8. Distribution of the area fraction of creep voids in HAZ of the thick plate welded joint of Mod.9Cr-1Mo steel during creep at 600 °C for 90 MPa.

4.4. Function f^* introduced in the two models

The function f^* is dependent on the combined effect of the stress triaxial factor and the equivalent creep strain during the progress of creep. At every time step, we can calculate its average along the weak HAZ on the basic of FE simulation, f^* in the weak HAZ of the thick and thin welded joint were plotted as shown in Fig. 9. The calculation shows that the average values of f^* increase with the creep time in the range from 1 to 1.16 for thick welded joint and 1–1.3 for thin welded joint. In the above sections, we always assumed that the function f^* was invariable, since variation in f^* does not affect the calculation of the creep time to rupture of welded joint with same groove shape. We introduced this function to evaluate the distribution of the localized damage along the weak HAZ. Therefore, the term Mf^* can be thought as invariable under a multiaxial stress state. The values of f^* for the thin welded joint during creep were higher than for the thick welded joint, which agrees with the observation that the creep time to rupture of the

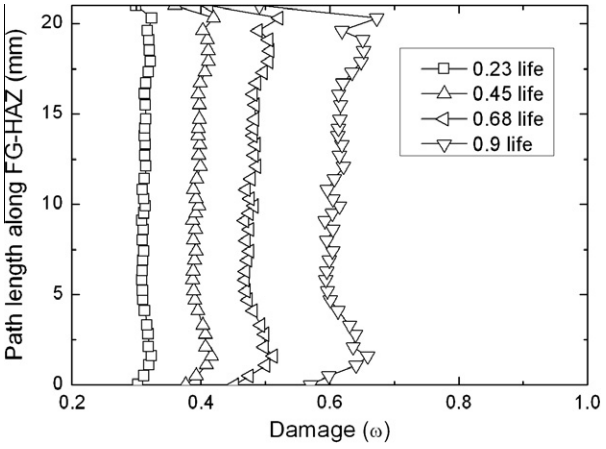

Fig. 7. Damage distribution of the thick welded joint along Path two during creep at 600 °C calculated with FEM.

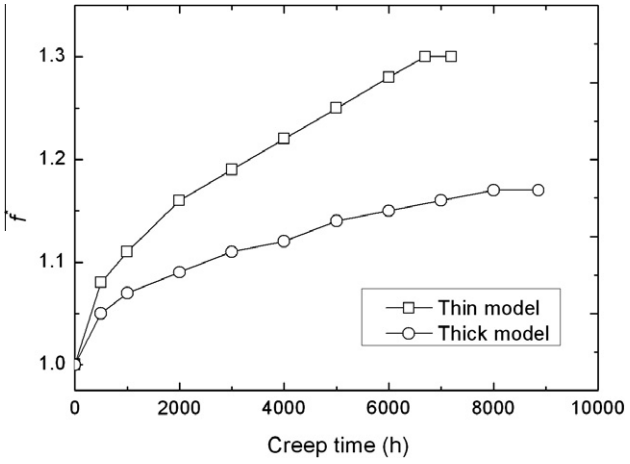

Fig. 9. Change in f^* with time in the models of thick and thin welded joint under 90 MPa at 600 °C.

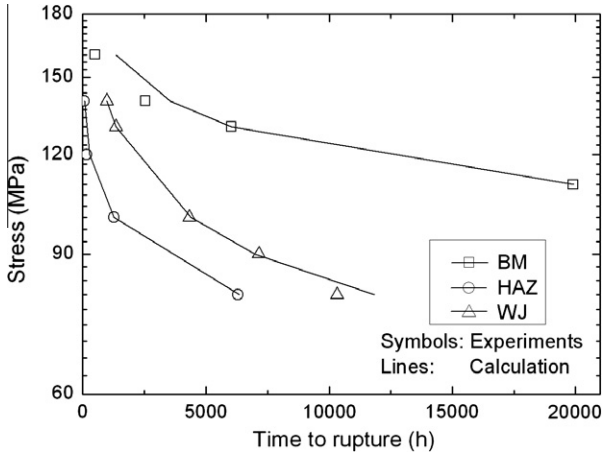

Fig. 10. Predicted and measured creep life BM, simulated HAZ and weldment at 600 °C.

thin welded joint is shorter than that of the thick welded joint. This also demonstrates the high reliability of f^*.

4.5. Creep life prediction

Fig. 10 compares our CDM calculations of the creep time to rupture with the measurements. Two parameter sets corresponding to the following stress levels were selected: 110/130 MPa, 80/100 MPa and 90/100 MPa, for BM, simulated HAZ and WJ respectively, and the predictions were close to the experimental results. Under the stress of 80 MPa for WJ and 160/140 MPa for BM, the predicted lives were longer than the measured lives. As we mentioned earlier, the material constants (A, n, χ and M) are invariable for given temperatures. However, long term service at high temperature would deteriorate the material, which is the reason why the creep life predictions for the BM, simulated HAZ and particularly the welded joint are higher than the measurements. The longer the service time is spent, the greater the difference between the prediction and experimental results will occur. The other exponents (of m and φ) varied according to the applied stress, but these have smaller effects on the predicted lives of the materials. The material constants of M and χ are scalar quantities, and at least one of them increases after the creep time reach a certain levels, because of the degradation of the materials due to the formation of large precipitation $Cr_{23}C_6$, Laves phase, and Z phase [19,20]. The change in the coefficient relations due to the material degradation can be clarified by conducting a set of second-time creep tests, in which the testing of specimens is interrupted for a certain time and then they are put into the same conditions as before. However, these changes might not be a function of time but rather of the applied stresses and temperatures in these evaluation equations.

The equivalent creep stress (σ_{eq}) ranged between 60% and 70% of the maximum principal stress in the thick model [14]. Thus, the effective stress ($\alpha\sigma_1 + (1-\alpha)\sigma_{eq}$) causing rupture used in the CDM equations was lower than the applied stress σ_0, due to the presence of multiaxial stress rupture criterion α in the conventional constitutive equations. However, substitution of the applied stress for the term ($\alpha\sigma_1 + (1-\alpha)\sigma_{eq}$) did not affect the prediction of rupture time for the weldment in the modified equations, because in addition the values of the related constants M and χ in the modified equations were different from the M and χ in the conventional constitutive equations. Therefore, the modification by substitution of ($\alpha\sigma_1 + (1-\alpha)\sigma_{eq}$) with σ_0 reasonably simplified the continuum damage mechanics constitutive equations.

5. Summary

A series of creep tests were conducted with specimens of BM, simulated HAZ and WJ at 600 °C, and primary creep damage taking the form of voids was observed in the thick welded joint, at the interruptions 0.1, 0.2, 0.5, 0.7, 0.8 and 0.9 of the rupture life under the stress of 90 MPa. A CDM approach based on results of experiments was used to evaluate the creep damage of a thick welded joint of Mod.9Cr–1Mo steel, with the aid of FEM simulation. The linear relations of the logarithms of m and $1/\lambda$ with the ratio of the applied stress to the yield stress of the homogeneous material were used to adjust the material constants. As creep coefficients are dependent on the applied stress, they reflect the normalized primary and secondary creep strain. The conventional evaluation equations for creep damage were modified by introducing a function f^* dependent on the combined effect of the equivalent creep strain and the stress triaxial factor. A function where the equivalent creep strain is an exponent of the stress triaxial factor was verified to be a very reliable factor for evaluating the damage in the complicated components. In this way, accurate creep damage evaluation of a thick welded joint under 90 MPa at 600 °C was conducted.

Acknowledgements

This work was supported in part by The Special Subsidies in Subsidies for ordinary expenses of private schools by the Promotion and Mutual Aid Corporation for Private Schools of Japan.

Present study also includes the results of the study "Development of damage prevention technology for welded structures in the next-generation high temperature nuclear plant" entrusted to Central Research Institute of Electric Power Industry by the Ministry of Education, Culture, Sports, Science and Technology of Japan (MEXT).

References

[1] S.J. Brett, D.J. Allen, J. Pacey, Failure of a modified 9Cr header endplate, in: CHIFI International Conference, Milan, September 1999, pp. 873–884.
[2] S.J. Brett, D.L. Oates, C. Johnston, In-service type IV cracking in a modified 9Cr (Grade 91) header, in: ECCC Creep Conference, London, September 2005, pp. 563–572.
[3] L.M. Kachanov, Izvestiya Akademii Nauk SSR Otdelenie Technicheskikh Nauk 8 (1958) 26–31.
[4] D.R. Hayhurst, P.R. Dimmer, M.W. Chernuka, J. Mech. Phys. Solids 21 (1973) 431–446.
[5] A.C.F. Cocks, M.F. Ashby, Metal Sci. (1980) 395–402.
[6] A.A. Becker, T.H. Hyde, W. Sun, P. Ansersson, Comput. Mater. Sci. 25 (2002) 34–41.
[7] S.T. Tu, R. Wu, R. Sandstrom, Int. J. Press. Vessel Pip. 58 (1994) 345–354.
[8] T. Yu, M. Yatomi, H.J. Shi, Int. J. Press. Vessel Pip. 86 (2008) 578–584.
[9] D.R. Hayhurst, J. Mech. Phys. 20 (1972) 381–390.
[10] T.H. Hyde, W. Sun, A.A. Becker, Int. J. Press. Vessel Pip. 78 (1991) 765–771.
[11] D.R. Hayhurst, P.R. Dimmer, C.J. Morrison, Math. Phys. Sci. 311 (1984) 103–129.
[12] F.R. Hall, D.R. Hayhurst, Roy Soc 433 (1995) 383–403.
[13] W.G. Kim, S.H. Kim, W.S. Ryu, Application of K–R creep damage model for type 316LN and HT-9 stainless steels, in: Japan Soc. Mech. Eng., Proc. of CREEP7. Tsukuba, January 2001, pp. 167–172.
[14] Y. Li, Y. Monma, H. Hongo, M. Tabuchi, Damage mechanics approach to evaluate creep voids leading to type IV cracking in Mod.9Cr–1Mo steel welded joint, in: Proceedings of The Six Asian Pacific IIW International Congress, Tianjin, China, October 10–13, 2008.
[15] M. Tabuchi, H. Hongo, Y.K. Li, T. Watanabe, Y. Takahashi, Proceedings of 2007 ASME Pressure Vessels and Piping Division Conference, San Antonio, Texas, July 2007, PVP2007-26495.
[16] Y.K. Li, H. Hongo, M. Tabuchi, Y. Monma, Int. J. Press. Vessel Pip. 86 (2008) 585–592.
[17] M. Tabuchi, H. Hongo, Y.K. Li, T. Watanabe, Y. Takahashi, J. Press. Vessel Technol. – Trans. ASME 131 (2) (2009).
[18] H. Hongo, M. Tabuchi, Y.K. Li, Y. Takahashi, J. Soc. Mater. Sci. Jpn. 58 (2009) 101–107 (in Japanese).
[19] K. Sawada, K. Miyahara, H. Kushima, K. Kimura, S. Matsuoka, JSME Int. J. 45 (2005) 1934–1939.
[20] K. Sawada, H. Kushima, K. Kimura, JSME Int. J. 46 (2006) 769–775.